Effect of Paeoniflorin on neurons autophagy and Notch expression of tether cord spinal in rats

Keywords
Paeoniflorin, Autophagy, Notch, Spine, Tethered cord, Spinal Disease

Abstract

Introduction

The study aimed to investigate the role of paeoniflorin in regulating neuronal autophagy and explore its ameliorative effects on the NOTCH signaling pathway in rat spinal cord tethering syndrome (TCS).

Material and methods

We conducted an experiment using 60 healthy male SD rats, randomly divided into six groups: Sham+Vehicle (saline) group; Sham+ Paeoniflorin (PF) 25mg/kg group; TCS+Vehicle group; TCS+PF25mg/kg group; TCS+PF50mg/kg group; TCS+PF100mg/kg group. We assessed neurological recovery by measuring Tarlov scores and Basso Beattie Bresnahan (BBB) scores at 1, 3, 7, 11, and 14 days after injecting PF. Additionally, we evaluated autophagic pathways, including LC3, Beclin1, and Notch protein expressions in rat spinal cord cells for each group.

Results

Lower limb neurological scores decreased after surgery on the first postoperative day. As the PF concentration increased, the recovery of Tarlov and BBB scores in rats accelerated. The comparison between PF treatment groups with different concentrations revealed a concentration-dependent effect. In the treated group, LC3 and Beclin1 protein expressions gradually decreased with increasing PF dose. Notch protein expression around spinal cord tissue significantly increased in the treated group of rats, while it was not significant in the control group (Sham, Sham+PF25mg/kg groups).

Conclusions

The results demonstrate that paeoniflorin can inhibit neuronal autophagy-related proteins and suppress apoptosis in spinal cord tissue. This inhibition contributes to improving neurological function in rats with tethered cord syndrome through the combined actions of autophagy inhibition and Notch pathway activation.

Effect of Paeoniflorin on neurons autophagy and Notch expression of tether cord spinal in rats

Feng Qingqi[1#], Li Jian[2#], Zhang Wenwen[2], Yu Chaochun[2*]

1. Longhua Hospital Affiliated to Shanghai University of Chinese Medicine Department of Neurosurgery
2. Shanghai TCM Integrated Hospital, Shanghai University of TCM, Department of Neurosurgery

Abstract

Objective: The study aimed to investigate the role of paeoniflorin in regulating neuronal autophagy and explore its ameliorative effects on the NOTCH signaling pathway in rat spinal cord tethering syndrome (TCS).

Method: We conducted an experiment using 60 healthy male SD rats, randomly divided into six groups: Sham+Vehicle (saline) group; Sham+ Paeoniflorin (PF) 25mg/kg group; TCS+Vehicle group; TCS+PF25mg/kg group; TCS+PF50mg/kg group; TCS+PF100mg/kg group. We assessed neurological recovery by measuring Tarlov scores and Basso Beattie Bresnahan (BBB) scores at 1, 3, 7, 11, and 14 days after injecting PF. Additionally, we evaluated autophagic pathways, including LC3, Beclin1, and Notch protein expressions in rat spinal cord cells for each group.

Results: Lower limb neurological scores decreased after surgery on the first postoperative day. As the PF concentration increased, the recovery of Tarlov and BBB scores in rats accelerated. The comparison between PF treatment groups with different concentrations revealed a concentration-dependent effect. In the treated group, LC3 and Beclin1 protein expressions gradually decreased with increasing PF

dose. Notch protein expression around spinal cord tissue significantly increased in the treated group of rats, while it was not significant in the control group (Sham, Sham+PF25mg/kg groups).

Conclusion: The results demonstrate that paeoniflorin can inhibit neuronal autophagy-related proteins and suppress apoptosis in spinal cord tissue. This inhibition contributes to improving neurological function in rats with tethered cord syndrome through the combined actions of autophagy inhibition and Notch pathway activation.

Key words: Paeoniflorin; Tethered cord; Autophagy; Notch; Spine; Spinal Disease

Introduction

Tethered cord syndrome (TCS) is a complex neurological condition that presents numerous challenges for both research and clinical management [1]. The condition is characterized by the spinal cord's abnormal fixation, leading to a variety of symptoms including urinary and defecation dysfunction, sensory disturbances, and pain [2–4]. While surgical intervention, such as tethered cord release (TCR), remains the primary treatment approach, there is a growing interest in exploring alternative and complementary therapies, particularly in the realm of traditional medicine [5].

Paeoniflorin (PF), a principal active constituent extracted from the peony root, has garnered significant attention due to its diverse pharmacological activities [6]. With established effects such as anti-inflammation, antioxidant properties, antispasmodic action, and immunomodulation [7]. PF presents a promising candidate for the treatment of neurological disorders, including TCS [8,9].

The anti-inflammatory effect of PF can be particularly beneficial in TCS, where inflammation can exacerbate nerve damage and contribute to the condition's progression. The antispasmodic effect of PF is crucial in alleviating the muscle spasms and abnormal neuronal excitability often seen in TCS patients. By reducing these symptoms, PF could improve the quality of life for individuals affected by the condition. Furthermore, the immunomodulatory effects of PF

could help regulate the immune system's response, thereby reducing inflammation and tissue damage.
Research has begun to uncover the specific mechanisms by which PF may exert its neuroprotective effects in TCS.

The development of accurate animal models is essential for advancing our understanding of TCS and for testing the efficacy of potential treatments such as PF . While various methods have been employed to create spinal cord tethered animal models, there is a need for models that closely mimic the clinical presentation of TCS [10]. By establishing evaluation standards that reflect the actual symptoms and outcomes of TCS, researchers can better assess the impact of treatments like PF on the neurological function of affected animals.
In summary, while surgical treatment remains the cornerstone of TCS management, the exploration of traditional Chinese medicine, particularly the use of PF, offers a promising avenue for potential therapeutic advancements. The multifaceted pharmacological activities of PF, combined with its neuroprotective properties, make it a compelling candidate for further research into the treatment of TCS. With continued investigation into the mechanisms of action and the development of more accurate animal models, the potential of PF in the management of TCS can be fully realized, offering new hope for patients suffering from this complex neurological condition.

2. Methods

2.1 Experimental subjects

All experiments in this study were approved by the Ethics Committee of Shanghai University of Traditional Chinese Medicine (PZSHUTCM220627035) and were conducted in accordance with the approval guidelines. 60 healthy male SD rats were selected, each with a growth age of about 6 to 8 weeks and 200 to 220 g. The rats were kept in cages with a constant temperature of 23±2°C and a prescribed 12-hour light/dark cycle. We provide special food for SD rats and sufficient clean drinking water. All experiments were conducted in accordance with the "Guidelines for the Care and Use of Laboratory Animals" (2006, Ministry of Science and Technology of China). All animal experiments conducted by the Animal Protection Committee of Shanghai University of Traditional Chinese Medicine are in compliance with the International Association for the Study of Pain Animal Research Guidelines as well.

2.2 Experimental modeling

In supplemental part.

2.3 Experimental animal grouping

SD rats were randomly divided into 3 groups: 6 rats in the control group Sham+Vehicle (physiological saline) and 6 rats in Sham+PF25mg/kg; the modeling group was divided into 12 rats in the control group TCS+Vehicle (physiological saline) and the treatment group TCS+PF25mg /kg, TCS+PF50mg/kg, TCS+PF100mg/kg).

2.4 Behavioral test

According to the weight of the rat, prepare different concentrations of PF and dissolve it in 0.9% physiological saline. The injection solution volume is 2 ml. Place it in a 2 ml syringe for intraperitoneal injection for 14 consecutive days. Neurological function scores (Tarlov score, BBB score) were performed on 1d, 3d, 7d, 11d, and 14d. After 14d, the rats in the four groups of TCS models were sacrificed and histological examination was taken.

2.5 Experimental drugs

Dissolve different doses of paeoniflorin in 2 ml of 0.9% normal saline and inject it into the abdominal cavity of rats with a 2 ml syringe. According to preliminary experiments and preliminary research results, PF (25 mg/kg, 50 mg/kg, 100 mg/kg) is the optimal dosage and has a concentration gradient effect. Starting from the first day after TCS modeling, PF or vehicle (physiological saline) was injected intraperitoneally once a day for 14 consecutive days.

2.6 Neurological function score

Referring to the method described by Sam et al [11], the hindlimb motor function was recorded and scored using the Tarlov scoring standard on 1d, 3d, 7d, 11d, and 14d

after TCS modeling in the control group and TCS modeling respectively, and the BBB scoring system was used to evaluate the later recovery (see Appendix B&C). (Assess the spinal nerve function of rats in each group. The data are collected in a blinded manner, in triplicate.) Supplementary righting reflex test and foot failure test were used to evaluate the sensory function of the lower limbs of rats. The righting reflex test was performed on days 1, 3, 7, 11, and 14. The rats were placed supine, and the time (s) for them to completely turn over and return to their natural position was recorded. The foot failure test was performed on days 1, 3, 7, 11, and 14. The rats were placed on the elevated grid surface, and the ratio of the number of footstep failures that occurred within 60 seconds was recorded.

2.7 Histological testing

The rats were sacrificed 14 days after TCS. The rat spinal cord tissue specimens were taken. The end of the filum terminale of the spinal cord was taken for pathology. The spine was taken out. A 5ml syringe was inserted into the spinal canal to blow out the spinal cord and filum terminale tissue. Pathology (HE and Nissl staining) was used, and Western blotting and immunohistochemistry techniques to detect spinal cord tissue.

2.8 Specimen collection

After the nerve injury of the rat, the score was completed and the rat was euthanized. The spinal cord tissue was extracted at the end of the conus spinal cord, washed, and subjected to routine dehydration, transparency, paraffin embedding, sectioning, and baking, and then fixed with 4% paraformaldehyde 96 hour, wash with PBS and seal in the refrigerator.

2.9 HE staining of rat spinal cord tissue

Rat spinal cord tissue was collected (the sample site included the tethered center), dewaxed with xylene and ethanol, stained with hematoxylin for 10 minutes, rinsed with

tap water for 5 minutes, differentiated with 1% hydrochloric acid alcohol, rinsed with tap water for 1 minute, and 1% Ammonia water returns to blue, rinse with tap water for 1 minute and then stain with eosin stain for 1 minute. Rinse with tap water for 1 minute and then clear with ethanol and xylene. After sealing with neutral gum, use an optical microscope for histopathological observation.

2.10 Nissl staining

Samples were taken from TCS model rats (the sample site included the entire tethering center), and the frozen sections were located at 3 mm from the tethering center and close to the tail of the spinal cord, with a thickness of 20 um. The frozen sections were air-dried at room temperature and then immersed in a mixed liquid (absolute ethanol: chloroform = 1:1) at room temperature overnight in a dark place. The next day, the tissues were placed in absolute ethanol, 95% alcohol, 70% alcohol and triple distilled water in sequence. Afterwards, it was stained with 0.05% tar violet, followed by 95% alcohol differentiation, 100% alcohol dehydration and xylene transparency treatment. Finally, it was sealed with neutral gum and the morphology and number of Nissl bodies were observed under a microscope.

2.11 Western blot detection

The most reagents for protein analysis was bought from Beyotime Biotechnology (Shanghai, China) except others were specified. Detection of autophagy-related protein levels in rat spinal cord tissue: Western blotting method was used to detect the protein expression levels of LC3 and Beclin1 (Santa Cruz, China). The spinal cord filum terminale tissue from each group was washed and minced, then 1 mL of RIPA lysis solution was added and ground into homogenate, and then homogenized on ice. Fully lyse for 10 minutes, centrifuge for 30 minutes at 4°C and 12,000 r/min, and then take the supernatant and measure it with the BCA method. First, take the supernatant of equal concentration and add an equal volume of loading buffer, and bathe in boiling water for

3 minutes, and configure the separation gel at the same time. After completion, electrophoresis is carried out with an electrophoresis instrument. It ends when the bromophenol blue reaches the edge of the gel. Then transfer the membrane for 1.5 hours. After washing the membrane, block it for 2 hours. Then dilute LC3 and Beclin1 according to the ratio of 1:1000. Antibody, add diluted primary antibody and incubate at 4°C overnight. After washing the membrane, add horseradish peroxidase secondary antibody diluted at 1:5000 and incubate at 37°C for 2 hours at room temperature with gentle shaking; after washing the membrane, use an ECL fluorescence kit Measure and calculate the relative expression levels of LC3 and Beclin1 proteins by calculating the ratio with β-Actin.

2.12 Immunofluorescence detection

Detection of Notch protein expression levels in rat spinal cord tissue: immunohistochemistry was used. Spinal cord tissue from each group was first taken, dewaxed for 1 hour, hydrated with ethanol gradient, washed 3 times with phosphate buffered saline (PBS), and then sodium citrate was added. Put it into a microwave oven for tissue antigen repair. The temperature of the microwave oven is 900°C, the heat is 60, and the repair time is 10 minutes. After cooling in the greenhouse, wash with PBS 3 times. Add 3% hydrogen peroxide methanol solution and incubate in the dark for 30 minutes. Wash with PBS 3 times. Then add diluted primary antibody (1:100), incubate at 4°C overnight, wash 3 times with PBS after warming, add biotin-labeled secondary antibody (1:500), incubate at room temperature for 60 min, wash 3 times with PBS, add diluted Third antibody (1:500), washed 3 times with PBS, developed with DAPI kit for 10 minutes, washed 3 times with tap water, dehydrated with graded ethanol, transparentized with xylene, sealed with center gum and observed under a microscope.

2.13 Statistical analysis

All data are expressed as mean ± standard deviation. SPSS25.0 (IBM, USA) was

used for data statistical analysis. One-way analysis of variance was used for comparison between two groups in the control group and among multiple groups in the TCS group. $p<0.05$ and $p<0.01$ are used as the criteria for judging significant and extremely significant differences respectively.

3. Results

3.1 TCS modeling results

Finally, 48 rats were successfully modeled and randomly divided into four groups (12 rats with TCS+Vehicle, 12 rats with TCS+PF25 mg/kg, 12 rats with TCS+PF 50 mg/kg, and 12 rats with TCS+PF100mg/kg). During the modeling process, no rats died in the last 14 days (Figure 1). After the rats woke up from anesthesia and went through a 1-day pain adaptation period, the spinal cord function was evaluated 24 hours later with a Tarlov score of 2 to 4, which belonged to TCS.

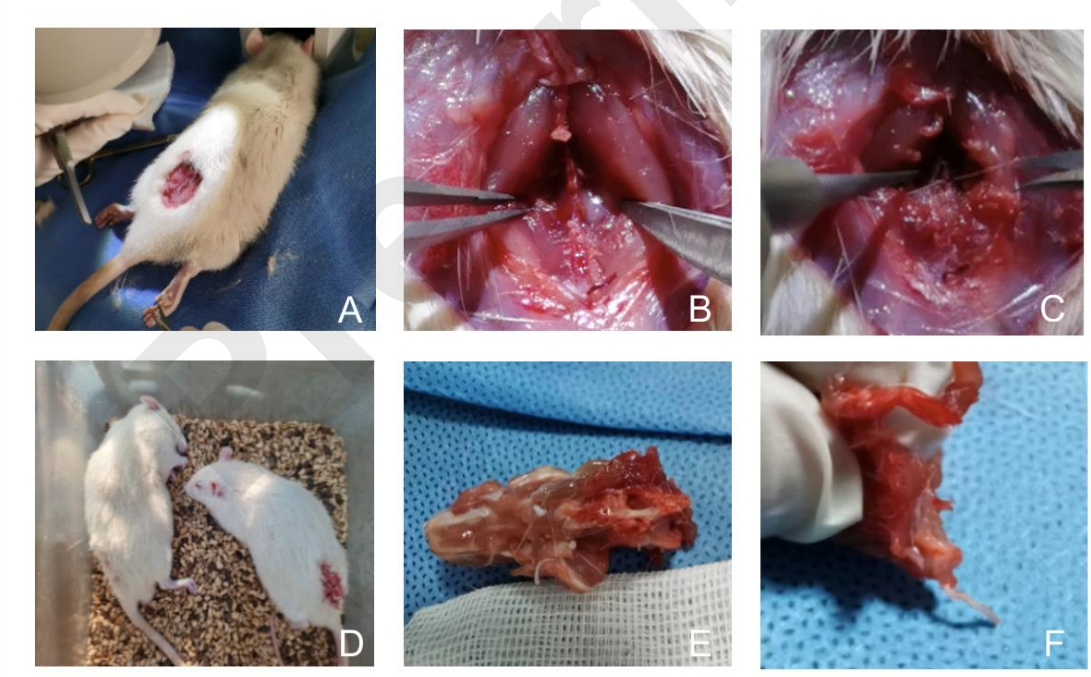

Fig 1 The rat TCS modeling procedure

3.2 Nervous function score of lower limbs in rats after TCS modeling

In the control group, there was no statistical difference between preoperative and postoperative Tarlov (Table 1) and BBB (Table 2) scores ($p>0.05$), however, in the modeling group, the Tarlov score 1 day after surgery ranged from 2.40±0.47 to 2.5±0.50, which is lower than the control group (*$p<0.05$). The BBB score 1 day after surgery in the modeling group ranged from 11.00±1.58 to 11.75±1.16, which was lower than that of the control group (*$p<0.05$), there was no statistical difference between the groups within the modeling group ($\Delta p>0.05$). As the experiment progressed, we observed that the Tarlov and BBB scores of rats in the TCS group gradually recovered (#$p<0.05$). In addition, the comparison between the TCS + PF groups of different concentrations in the modeling group showed concentration dependence, that is, the higher the PF concentration was given to the rats, the more obvious the recovery of their lower limb nerve functions was (Figure 2&3).

Table 1 Tarlov score after control group and TCS modeling ($\bar{x}$±s)

	Sham+Vehicle (n=6)	Sham+PF25mg/kg (n=6)	TCS+Vehicle (n=12)	TCS+25mgPF (n=12)	TCS+PF50mg/kg (n=12)	TCS+PF100 mg/kg (n=12)
1d	5.00±0.00	5.00±0.00	2.50±0.50$^{\Delta}$	2.40±0.47$^{\Delta}$	2.40±0.47$^{\Delta}$	2.50±0.50$^{\Delta}$
3d	5.00±0.00	5.00±0.00	2.6±0.49*	2.70±0.47*$^{\#}$	2.80±0.37*$^{\#}$	3.20±0.69*$^{\#}$
7d	5.00±0.00	5.00±0.00	2.90±0.76*	3.10±0.76*$^{\#}$	3.20±0.69*$^{\#}$	3.50±0.87*$^{\#}$
11d	5.00±0.00	5.00±0.00	3.17±0.37*	3.17±0.69*$^{\#}$	3.67±1.04*$^{\#}$	4.25±0.72*$^{\#}$
14d	5.00±0.00	5.00±0.00	3.65±0.94*	3.70±0.94*$^{\#}$	3.90±1.04*$^{\#}$	4.33±0.75*$^{\#}$

Note: Comparison of variances between groups after 1 day of modeling, $\Delta p>0.05$, there is no statistical difference in postoperative Tarlov scores of rats in each group. Comparison of 3d, 7d, 11d, 14d between the modeling group and the control group *$p<0.05$; Comparison between TCS+Vehicle and TCS+PF administration groups in the modeling group, #$p<0.05$; Sham and Sham+PF25mg/kg in the control group $p>0.01$ between groups, there is no statistical difference between the two groups.

Table 2: BBB scores after control group and TCS modeling ($\bar{x}$±s)

	Sham+Vehicle (n=6)	Sham+PF25mg/kg (n=6)	TCS+Vehicle (n=12)	TCS+25mg PF (n=12)	TCS+PF50mg/kg (n=12)	TCS+PF 100mg/kg (n=12)
1d	20.00±0.00	20.00±0.00	11.00±1.58$^{\Delta}$	11.75±1.16$^{\Delta}$	11.42±1.18$^{\Delta}$	11.42±1.26$^{\Delta}$

3d	20.00±0.00	21.00±0.00	11.67±1.49*	10.94±0.91*#	11.42±1.19*#	12.00±1.46*#
7d	21.00±0.00	21.00±0.00	13.67±1.11*	13.64±1.11*#	13.50±0.76*#	15.83±0.95*#
11d	21.00±0.00	21.00±0.00	12.92±1.11*	14.00±1.55*#	15.60±1.61*#	16.00±0.80*#
14d	21.00±0.00	21.00±0.00	14.17±1.49*	15.08±1.55*#	16.50±1.18*#	18.17±0.99*#

Note: Comparison of variances between groups after 1 day of modeling, Δp>0.05, there was no statistical difference in postoperative BBB scores of rats in each group. Comparison between the modeling group and the control group at 3-14 days *p< 0.05; Comparison between the TCS+Vehicle and TCS+PF administration groups in the modeling group, #p< 0.05, there is a statistical difference. In the control group, Sham and Sham+PF25mg, p>0.05, no statistical difference.

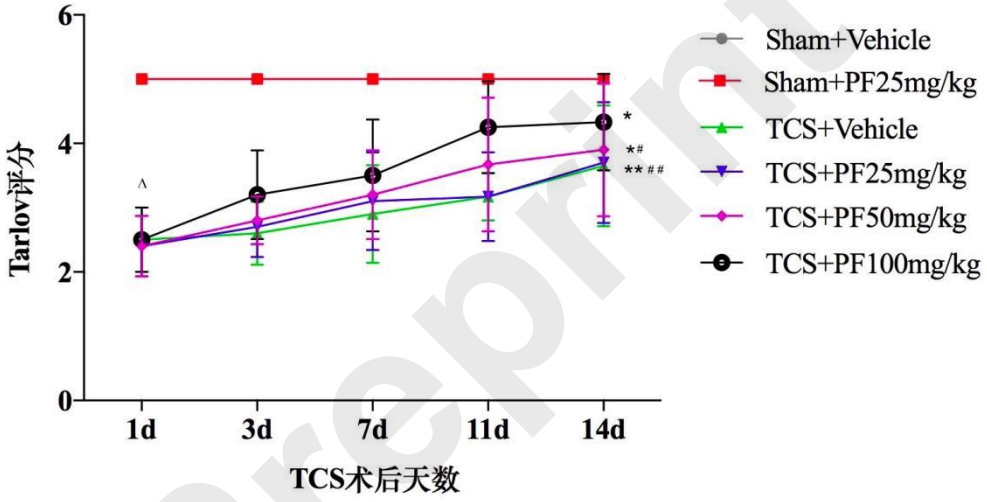

Figure 2: Comparison of the mean and variance of Tarlov scores of SD rats in two non-surgical groups and four modeling groups 1d, 3d, 7d, 11d, and 14d after treatment.

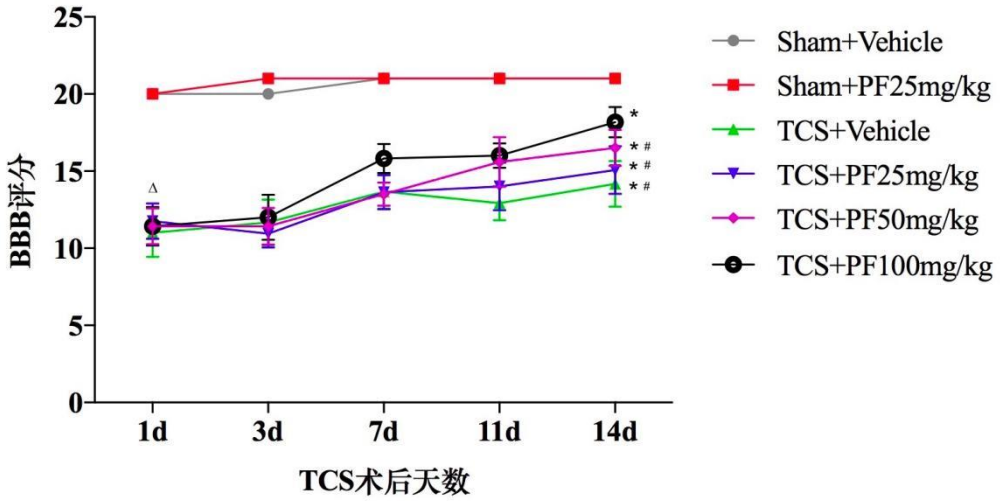

Figure 3: Comparison of the mean and variance of BBB scores of two non-surgical groups and four modeling groups of SD rats 1d, 3d, 7d, 11d, and 14d after treatment.

In the supplementary experiment, 3 rats from each group were selected for the righting reflex test and foot failure test on days 1, 3, 7, 11, and 14. In Table 3, there is no statistical difference between the preoperative and postoperative righting reflex test of the control group and the righting reflex test of the control group 1 d after surgery ($p>0.05$).

In the modeling group, the righting reflex test one day after surgery ranged from 11.15±0.92 to 11.40±0.34, which was higher than that of the control group ($p<0.05$). There is no statistical difference between the modeling groups on the 1st day after surgery ($\Delta p>0.05$). As the experiment progressed, we observed that the righting reflex test time of the control group rats in the TCS group gradually shortened ($p<0.05$). There were statistically significant differences between the four modeling groups and the drug administration group on days 3, 7, 11, and 14 ($*p < 0.05$). In the modeling group, there was a statistical difference between the TCS+Vehicle and TCS+PF groups $\#p<0.05$; Similarly, in Table 4, in the control group, the rate of rat footstep errors before and after surgery, and after surgery There was no statistical difference in the footstep error rate of rats in the control group on day 1 ($p>0.05$), indicating that PF had no effect on the movement sensation of rats in the control group.

In the modeling group, the righting reflex test one day after surgery ranged from 11.15±0.92 to 11.40±0.34, which was higher than that of the control group ($p<0.05$).

This shows that the nerve function of the lower limbs of rats is damaged to a certain extent after TCS modeling. As the experiment progressed, we observed that the rate of footstep errors in the control group of rats in the TCS group gradually decreased ($p<0.05$). There were statistically significant differences between the four modeling groups and the drug administration group on days 3, 7, 11, and 14 (*$p < 0.05$). In the modeling group, there was a statistical difference between the three groups of TCS+Vehicle and TCS+PF #$p<0.05$;

Table 3 Correction time after surgery in the control group and TCS modeling ($\bar{x}$±s)（s）

	Sham+Vehicle (n=3)	Sham+PF25 mg/kg (n=3)	TCS+Vehicle (n=3)	TCS+25mgPF (n=3)	TCS+PF50mg/kg (n=3)	TCS+PF100mg/ kg (n=3)
1d	1.50±0.08	1.51±0.09	11.27±0.95$^{\Delta}$	11.40±0.34$^{\Delta}$	11.32±0.87$^{\Delta}$	11.15±0.92$^{\Delta}$
3d	1.50±0.08	1.48±0.08	10.23±0.34*$^{\#}$	9.8±0.59*$^{\#}$	8.03±0.22*	5.80±0.71*$^{\#}$
7d	1.53±0.10	1.50±0.09	9.5±0.74*$^{\#}$	8.6±0.43*$^{\#}$	5.00±0.44*	3.12±0.62*$^{\#}$
11d	1.49±0.09	1.53±0.09	7.55±0.73*$^{\#}$	6.95±0.64*$^{\#}$	4.32±0.43*	2.18±0.43*$^{\#}$
14d	1.52±0.10	1.51±0.10	6.9±0.74*$^{\#}$	6.15±0.58*$^{\#}$	3.95±0.33*	2.03±0.26*$^{\#}$

Note: Comparison of variances between groups after 1 day of modeling, $\Delta p>0.05$, there is no statistical difference between groups. Comparison of 3d, 7d, 11d, and 14d between the modeling group and the control group *$p< 0.05$; Comparison of TCS+Vehicle and TCS+PF administration groups in the modeling group, #$p< 0.05$; Sham and Sham+PF25mg/kg in the control group $p>0.05$ between groups, no statistical difference.

Table 4: Footstep error rates in the control group and after TCS modeling ($\bar{x}$±s)（%）

	Sham+Vehicle (n=3)	Sham+PF25mg /kg (n=3)	TCS+Vehicle (n=3)	TCS+25mgPF (n=3)	TCS+PF50mg/k g (n=3)	TCS+PF100mg/kg (n=3)
1d	16.23±1.34	15.76±2.47	40.81±2.29$^{\Delta}$	41.96±0.87$^{\Delta}$	39.69±2.38$^{\Delta}$	40.12±1.23$^{\Delta}$
3d	16.04±1.78	15.97±1.95	35.76±3.51*	27.80±2.00*$^{\#}$	25.62±3.56*$^{\#}$	23.32±5.43*$^{\#}$
7d	16.19±2.23	16.19±2.15	31.49±3.11*	25.55±2.06*$^{\#}$	23.27±5.26*$^{\#}$	21.70±3.28*$^{\#}$
11d	15.90±1.46	15.74±1.75	26.14±4.01*	22.45±4.75*$^{\#}$	21.27±4.27*$^{\#}$	19.23±3.12*$^{\#}$
14d	15.34±1.76	16.12±1.53	23.12±2.85*	20.20±4.69*$^{\#}$	19.76±4.75*$^{\#}$	17.53±2.78*$^{\#}$

Note: Comparison of variances between groups after 1 day of modeling, $\Delta p>0.05$, no statistical significance.

Comparison of the modeling group on 3d, 7d, 11d, and 14d with the control group *p< 0.05; Comparison of TCS+Vehicle and TCS+PF administration group in the modeling group, #p< 0.05, statistically significant; 1d, 3d, 7d , p>0.05 between Sham and Sham+PF25mg/kg groups in the 11d and 14d control groups, with no statistical difference.

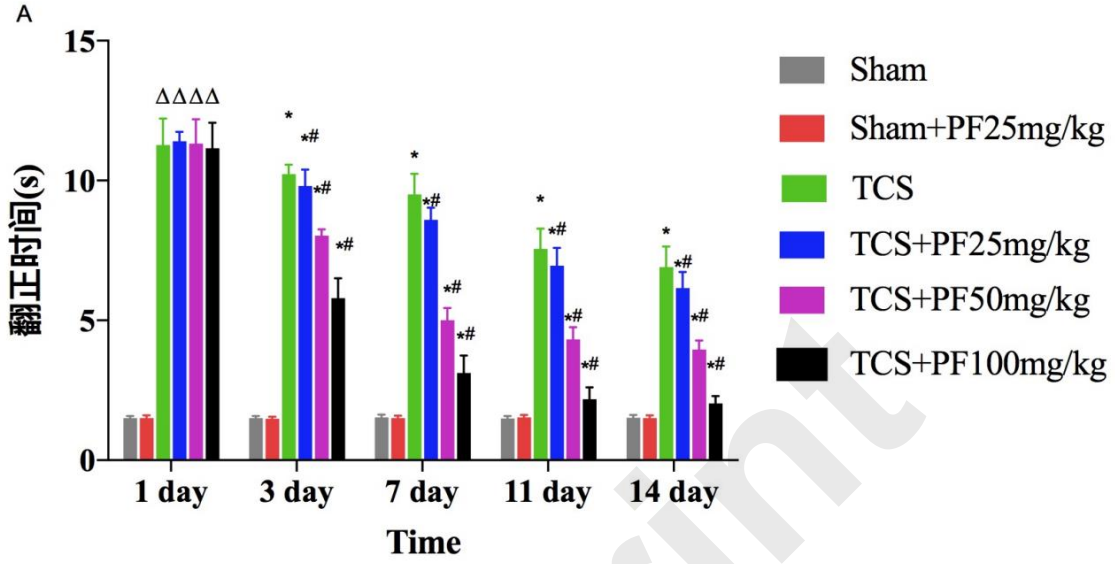

Fig 4：Comparison of the mean and variance of the righting time of SD rats in two non-surgical groups and four modeling groups on 1d, 3d, 7d, 11d, and 14d after treatment.

Note: Comparison of the righting time (s) of the control group and the modeling group on 1d, 3d, 7d, 11d, and 14d: Comparison of the modeling group on 1d, 3d, 7d, 11d, and 14d with the control group *p < 0.05; Modeling Comparison between TCS+Vehicle and TCS+PF administration groups, #p<0.05

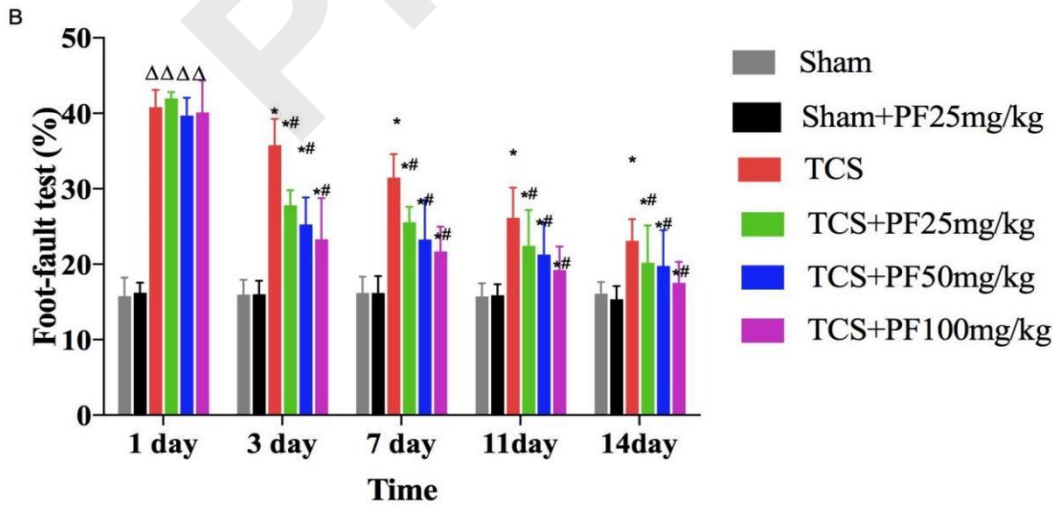

Figure 5: Comparison of the mean and variance of the righting time of SD rats in two non-surgical groups and four

modeling groups 1d, 3d, 7d, 11d, and 14d after treatment.

Note: Comparison of the righting time (s) of the control group and the modeling group on 1d, 3d, 7d, 11d, and 14d: Comparison of the modeling group on 1d, 3d, 7d, 11d, and 14d with the control group *p < 0.05; Modeling Comparison between TCS+Vehicle and TCS+PF administration groups, #p<0.05

3.4 Pathological changes

HE staining: In the control group, the structure of spinal cord nerve cells is intact, the morphology of the cell nuclei is normal and complete, the nucleoli are clear and neatly arranged, and there is no edema in the spaces around the cells; in the TCS group and TCS+PF treatment group, the spinal cord tissue and cortical structure are basically intact; the cell arrangement is slightly disorder, the nucleolar structure is partially intact, and fragmented cell cytoplasm can be seen.

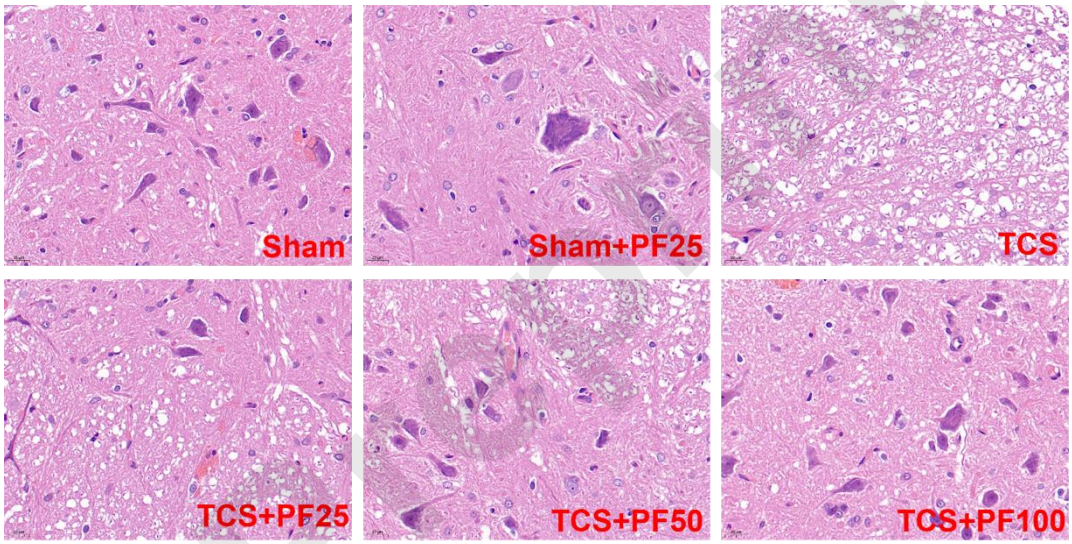

Figure 4. HE staining of spinal cord tissue (*400 times) A is the control group, B is the TCS group, C is the TCS+PF treatment group. D is the control group, E is the TCS group, and F is the TCS+PF treatment group.

Nissle staining: Nissl bodies are larger and more numerous in the control group. Nissl bodies were smaller in size and in number in the TCS group and TCS+PF treatment group. Mild damage to spinal cord nerve cells was found in the control group and TCS+PF treatment group, but there was little pathological difference between the modeling groups (Figure 5).

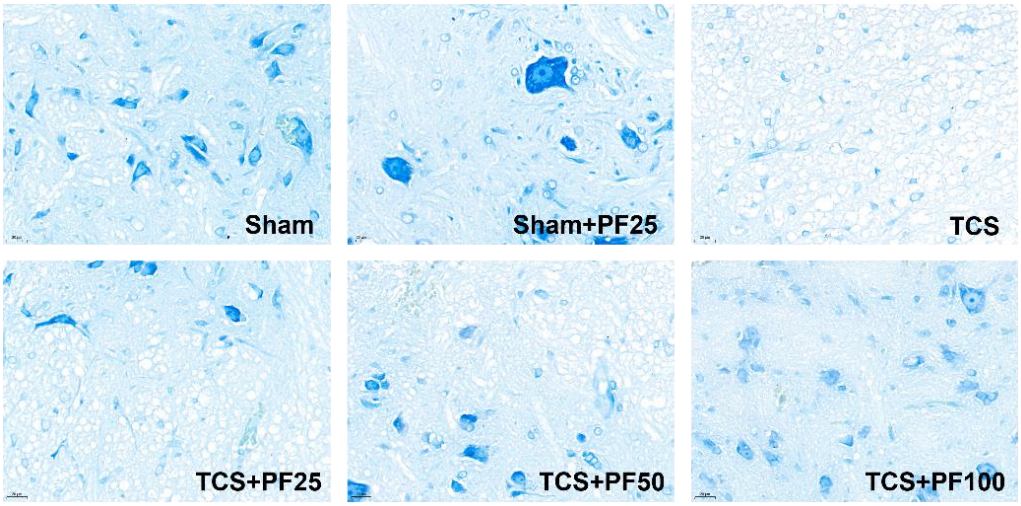

Figure 5. Nissl staining of spinal cord tissue (*400 times) in each group.

3.5 Western blot results

According to the relative expression content of LC3 (total amount of LC3I and LC3II) and Beclin1 protein, there was no statistical difference between the control group and the intra-group comparison of the TCS modeling group. Compared with the TCS group, the TCS+PF25mg/kg group, TCS+PF50mg/ kg group, TCS+PF100mg/kg group, the relative expression levels of LC3 and Beclin1 proteins decreased and were statistically different (#p <0.05). Compared with the control group, the TCS group, TCS+PF25mg/kg group, TCS+PF50mg /kg group, TCS+PF100mg/kg group, the average protein expression content increased and there was a statistical difference (*p <0.05). Comparison between TCS treatment groups found that with the increase of PF dose, the protein expression of LC3 and Beclin1 in rat spinal cord tissue gradually decreased (Table 5).

Table 5 Grayscale reference values of LC3, Beclin1 and β-Actin protein expression in tissue Western blot

	Sham+Vehicle	Sham+PF25mg/kg	TCS+Vehicle	TCS+25mgPF	TCS+PF50mg/kg	TCS+PF100mg/kg
β-Actin	3265030	3105660	2980044	3197077	3156749	3272472
	3267056	3105204	2976710	3191450	3144998	3277209
	3270314	3122918	2969530	3195683	3141757	3269005
Beclin1	1605043	1415723	2712441	2645230	2481969	2186881
	1613024	1575411	2807388	2729915	2358781	2112620
	1552710	1434733	2674927	2645620	2446083	2014633

LC3	1383716	1423003	2734319	1980681	1787047	1521006
	1481700	1341198	2678635	2103385	1800009	1572072
	1493065	1469515	2679545	2167789	1682035	1502768

Table 6: Expression ratio of LC3, Beclin1 and β-Actin proteins in WB (%)

	Sham+Vehicle	Sham+PF25mg/kg	TCS+Vehicle	TCS+25mgPF	TCS+PF50mg/kg	TCS+PF100mg/kg
Beclin1/β-Actin	0.49	0.46	0.91	0.83	0.79	0.67
	0.49	0.51	0.94	0.86	0.75	0.64
	0.47	0.46	0.90	0.83	0.78	0.62
LC3/β-Actin	0.42	0.46	0.92	0.62	0.57	0.46
	0.45	0.43	0.90	0.66	0.57	0.48
	0.46	0.47	0.90	0.68	0.54	0.46

Note: Comparison between the four modeling groups and the control group, *p< 0.05; Comparison between

the TCS+Vehicle and TCS+PF administration groups in the modeling group, #p< 0.05

Table 7: LC3、Beclin1 与 β-Actin protein expression ratio ($\bar{x}$±s)（%）

	Sham+Vehicle (n=3)	Sham+PF25mg/kg (n=3)	TCS+Vehicle (n=3)	TCS+25mgPF (n=3)	TCS+PF50mg/kg (n=3)	TCS+PF 100mg/kg (n=3)
Beclin1/β-Actin	0.48±0.01	0.47±0.03	0.91±0.02*	0.84±0.02*#	0.77±0.02*#	0.64±0.03*#
LC3/β-Actin	0.44±0.02	0.45±0.02	0.90±0.01*	0.65±0.03*#	0.56±0.02*#	0.46±0.01*#

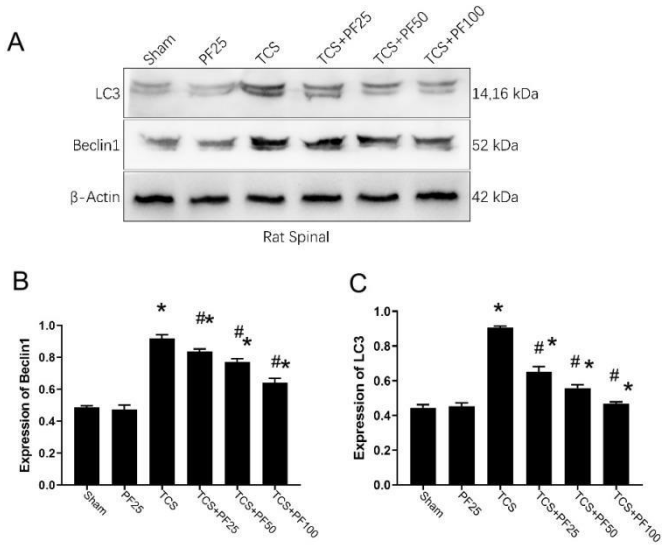

Figure 7 A: Western blotting results of LC3 (total amounts of LC3I and LC3II) and Beclin1 in different groups; B and C are the relative expression levels of LC3 and Beclin1 proteins as compared to β-Actin. Note: Compared with the control group, *p <0.05, compared with the TCS group, #p <0.05.

3.5 Immunofluorescence results

Compared with the TCS group, the apoptosis in the TCS+PF25mg/kg group, TCS+PF50mg/kg group, and TCS+PF100mg/kg group had a decrease trend and statistical difference (#p <0.05). While compared with the control group, both the TCS group and TCS+PF25mg/kg group were statistically different (*p <0.05). In the TCS modeling group, the nuclei of the cells are fragmented. The crack was incomplete, and the expression of Notch protein around the spinal cord tissue of rats in the TCS model groups (TCS group, TCS+PF25mg/kg group, TCS+PF50mg/kg group, TCS+PF100mg/kg group) increased significantly. In Sham + PF25 mg/kg group, the expression of Notch protein around the spinal cord cells was not obvious. However, when comparing with the TCS model groups, the expression of Notch in the TCS + Vehicle group was the mostly obvious. As the concentration of PF increases, the expression of Notch protein around the nucleus of spinal cord cells in the model group significantly decreases, indicating that PF has a significant inhibitory effect on Notch in the spinal cord tissue of TCS rats, and the higher the concentration of PF, the greater the inhibitory effect on Notch protein.

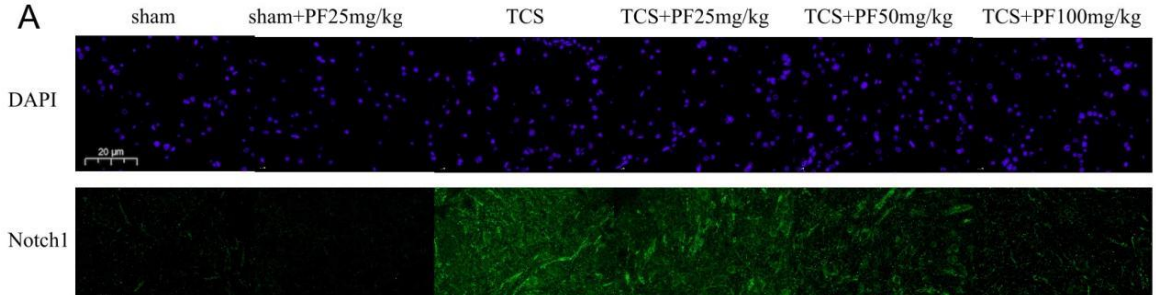

Figure 8　The effect of PF on the apoptosis rate in TCS rat spinal tissue.（IFC 40x）

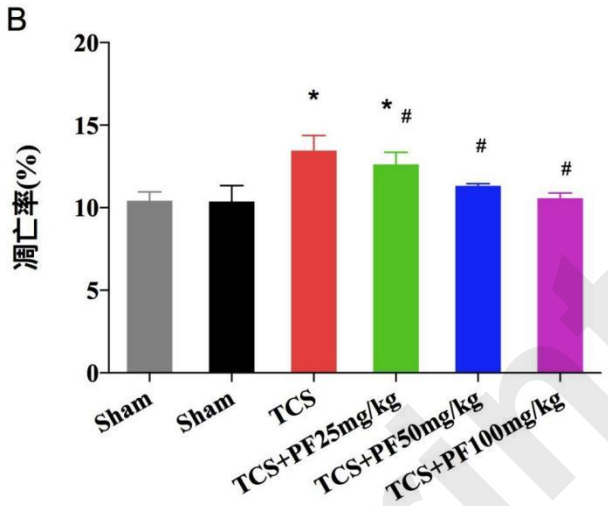

Figure 9 Results of PF directional analysis of cell apoptosis rate in spinal cord tissue of TCS rats:

Note: *p <0.05, compared with TCS group #p <0.05.

4.Discussion

4.1 Pathophysiology of tethered cord syndrome

Tethered Cord Syndrome (TCS) is a complex condition characterized by a constellation of neurological, urological, musculoskeletal, and gastrointestinal symptoms, with an incidence estimated at 0.25 per 1,000 individuals [12]. TCS onset is often triggered by a threshold of mechanical tension or by the cumulative effects of repetitive, transient strains [1]. Progressively, spinal cord blood flow diminishes due to ischemic injury, and the dysfunction of neuronal mitochondrial terminal oxidase ensues [13], culminating in disruptions to mitochondrial oxidative phosphorylation and electrophysiological homeostasis [14,15]. According to Yamada's research, a malfunction in the electron transport chain of neuronal mitochondrial terminal oxidase impairs efficient adenosine triphosphate (ATP) generation, which may contribute to cellular dysfunction in both human and experimental TCS models [16]. Hence, the development of a rat model of spinal cord tethering is anticipated to mimic chronic spinal cord traction injuries [17–19].

4.2 Pharmacological properties of paeoniflorin

Paeoniflorin (PF) is a bioactive compound extracted from the traditional Chinese herb Paeonia lactiflora. Its pharmacological attributes include: 1)Anti-inflammatory Activity: PF exhibits potent anti-inflammatory properties, inhibiting the production of inflammatory mediators such as TNF-α, IL-1β, and IL-6 [7]; 2) Antioxidant Properties: PF demonstrates significant antioxidant activity, scavenging free radicals, and attenuating oxidative stress-induced cellular damage [8]; 3)Anti-spasmodic Effects: PF can mitigate epileptic seizures by modulating neurotransmitter release and ion channel activity, thus dampening aberrant neural excitability [6]; 4)Analgesic Effects: PF shows potential in treating inflammatory pain by reducing the production of inflammatory mediators and neurotransmitter release [9]; 5) Immunomodulatory Actions: PF suppresses immune cell activation and inflammatory factor production, thereby modulating immune response balance and reducing immune-mediated inflammation and tissue damage [7].

4.3 Analysis of Western Blot Results

Our analysis revealed that, compared to the control group, the expression levels of autophagy-related proteins LC3 and Beclin1 were significantly elevated in the spinal cord tissue of SD rats with induced TCS ($P<0.05$). This suggests successful TCS modeling and a resultant increase in autophagy protein markers [20]. Treatment with various doses of PF resulted in a dose-dependent decrease in LC3 and Beclin1 expression ($P<0.05$), indicating that PF can mitigate autophagy-related protein upregulation and alleviate inflammation in spinal cord tissue [21,22].

4.4 Immunofluorescence Notch protein expression analysis

Preliminary experiments indicated that PF's therapeutic effects in TCS might involve the inhibition of the Notch signaling pathway. Following TCS induction, Notch1 protein expression was significantly elevated in rat spinal cord tissue. PF treatment led to a concentration-dependent decrease in Notch protein expression. Given that Notch signaling can impede neurological repair and exacerbate post-injury symptoms, PF's ability to reduce Notch protein expression suggests its potential role in inhibiting neuronal apoptosis and promoting neurological function recovery by modulating this pathway.

Conclusion

This study successfully established a rat model of spinal cord tethering and investigated the intervention effects of paeoniflorin. The results indicate that PF can inhibit neuronal autophagy-related proteins and apoptosis in spinal cord tissue, suggesting its neuroprotective role. Rat models demonstrated improved lower limb neurological function, supporting PF's efficacy in ameliorating symptoms of tethered spinal cord syndrome and highlighting the Notch pathway as a theoretical basis for the application of traditional Chinese medicine constituents in TCS treatment.

Conflict of Interest

The authors indicate that they do not have conflict of interest.

Funding: This project was supported by Shanghai Hongkong Health Committee, Traditional Chinese Medicine Project (HKQGYQY-ZYY-2022-01).

Abbreviations

Abbreviations	Full Name
BBB	Basso-Beattie-Bresnahan rating scale
CCI	Chronic constrictive injury
DAPI	4',6-diamidino-2-phenylindole
DAPT	γ -secretase blocker
GPCR	G protein coupled receptor
JAK/SATA	janus kinase/signal transducer and activator of transcription
LPS	lipopolysaccharide
M1/2 cell	Macrophages1/2
NF-κB	nuclear factor kappa-B
NLRP3	NOD-like receptor protein 3
PF	Paeoniflorin
PBS	Phosphate Buffer Saline
ROS	reactive oxygen species
SCS	Spinal Cord shortening
TCS	Tethered Cord Syndrome
TCR	Tethered Cord Release

TNF-α	Tumor Necrosis Factor-α
IL-1β	Interleukin-1 beta
LPS	lipopolysaccharide

References

1. Klinge PM, Leary OP, Allen PA, Svokos K, Sullivan P, Brinker T, et al. Clinical criteria for filum terminale resection in occult tethered cord syndrome. J Neurosurg: Spine. 2024;1–9.

2. Jiao L, Wang S, Yang X, Ma J, Zheng L, Wang H, et al. Current Global Research Trends of Tethered Cord Syndrome Surgery: A Scientometric and Visual Analysis. World Neurosurg. 2024;183:206–13.

3. Zheng P, Zhang N, Ren D, Yu C, Zhao B, Bai Q, et al. Integrated single-cell multiomics reveals novel immune candidate markers for post-traumatic coagulopathy. Front Immunol. 2023;13:1095657.

4. Zheng P, Zhang N, Ren D, Yu C, Zhao B, Zhang Y. Integrated spatial transcriptome and metabolism study reveals metabolic heterogeneity in human injured brain. Cell Reports Medicine. 2023;101057.

5. Kim S-G, Park J-H, Park H-B, Yoo D-H, Jang W-S, Shin W-B, et al. Filum Terminale Lipoma with Herniated Intervertebral Disc Treated with Traditional Korean Medicine: A Case Report. J Acupunct Res. 2020;37:281–4.

6. Fang X, Ji Y, Li S, Wang L, He B, li B, et al. Paeoniflorin attenuates cuproptosis and ameliorates left ventricular remodeling after AMI in hypobaric hypoxia environments. J Nat Med. 2024;1–13.

7. Yang J, Wei Z, Li H, Lv S, Fu Y, Xiao L. Paeoniflorin inhibits the inflammation of rheumatoid arthritis fibroblast-like synoviocytes by downregulating hsa_circ_009012. Heliyon. 2024;e30555.

8. Hu M, Wang A, Zhao Z, Chen X, Li Y, Liu B. Antidepressant-like effects of paeoniflorin on post-stroke depression in a rat model. Neurol Res. 2019;41:446–55.

9. Peng W, Chen Y, Tumilty S, Liu L, Luo L, Yin H, et al. Paeoniflorin is a promising natural monomer for neurodegenerative diseases via modulation of Ca2+ and ROS homeostasis. Curr Opin Pharmacol. 2022;62:97–102.

10. McElroy A, Klinge PM, Sledge D, Donahue JE, Glabman RA, Rashmir A. Evaluation of the Filum Terminale in Hereditary Equine Regional Dermal Asthenia. Vet Pathol. 2021;58:1100–6.

11. Safavi-Abbasi S, Mapstone TB, Archer JB, Wilson C, Theodore N, Spetzler RF, et al. History of the current understanding and management of tethered spinal cord. J Neurosurg Spine. 2016;25:78–87.

12. Bhimani AD, Selner AN, Patel JB, Hobbs JG, Esfahani DR, Behbahani M, et al. Pediatric tethered cord release: an epidemiological and postoperative complication analysis. J Spine Surg. 2019;5:337–50.

13. Thompson EM, Strong MJ, Warren G, Woltjer RL, Selden NR. Clinical significance of imaging and histological characteristics of filum terminale in tethered cord syndrome. J Neurosurg Pediatr. 2014;13:255–9.

14. Leary OP, Hagan M, Sullivan PLZ, McElroy A, Syed S, Liu DD, et al. Adult-Onset tethered cord Syndrome: Case series from a comprehensive interdisciplinary spine center. Interdiscip Neurosurg. 2023;33:101773.

15. Al-Askary SB, El-Kheir MMA, Mousa AE-HA. SURGICAL MANAGEMENT OF TETHERED CORD SYNDROME. Al-Azhar Méd J. 2022;51:891–904.

16. Yamada S, Won DJ, Pezeshkpour G, Yamada BS, Yamada SM, Siddiqi J, et al. Pathophysiology of tethered cord syndrome and similar complex disorders. Neurosurg Focus. 2007;23:1–10.

17. Zhang Z, Sui R, Xia D. A variant in microRNA-124 is involved in the control of neural cell apoptosis and associated with recovery after spinal cord injury (SCI). Arch Méd Sci : AMS. 2022;18:1399–403.

18. Chen L, Li X, Zhu J, Xu B, Gu Y. miRNA-19a exerts an anti-apoptotic effect in spinal cord injured rats via the PTEN pathway. Arch Méd Sci : AMS. 2019;19:744–56.

19. Chuan YM, Wang Y, Jin X, Ming SQ, Bing WW, Kai W, et al. Activation of CREB-binding protein ameliorates spinal cord injury in tabersonine treatment by suppressing NLRP3/Notch signaling. Arch Méd Sci : AMS. 2019;19:736–43.

20. Chen W, Guo Y, Yang W, Zheng P, Zeng J, Tong W. Involvement of autophagy in connexin 40 reduction in the late phase of traumatic brain injury in rats. Brain research bulletin. 2017;131:100–6.

21. Li S, Du J, Gan H, Chen J, Zhou Y, Tian J, et al. Resveratrol promotes apoptosis and G2/M cell cycle arrest of fibroblast-like synoviocytes in rheumatoid arthritis through regulation of autophagy and the serine-threonine kinase-p53 axis. Arch Méd Sci : AMS. 2021;20:280–8.

22. Ma L, Gao J. Suppression of lncRNA-MALAT1 activity ameliorates femoral head necrosis by modulating mTOR signaling. Arch Méd Sci : AMS. 2020;20:612–7.